

Cite this: *Analyst*, 2012, **137**, 4045

www.rsc.org/analyst

PAPER

Exploring the coordination chemistry of isomerizable terpyridine derivatives for successful analyses of *cis* and *trans* isomers by travelling wave ion mobility mass spectrometry†

Jonnatan J. Santos,^a Sergio H. Toma,^{*,a} Priscila M. Lalli,^b Maria F. Riccio,^b Marcos N. Eberlin,^b Henrique E. Toma^a and Koiti Araki^{*,a}

Received 6th March 2012, Accepted 18th June 2012

DOI: 10.1039/c2an35320b

The photochemical *cis*–*trans* isomerization of the 4-{4-[2-(pyridin-4-yl)ethenyl]phenyl}-2,2':6',2''-terpyridine ligand (vpytpy) was investigated by UV-vis, NMR and TWIM-MS. Ion mobility mass spectrometry was performed pursuing the quantification of the isomeric composition during photolysis, however an in-source *trans*-to-*cis* isomerization process was observed. In order to overcome this inherent phenomenon, the isomerization of the vpytpy species was suppressed by complexation, reacting with iron(II) ions, and forming the [Fe(vpytpy)₂]²⁺ complex. The strategy of “freezing” the *cis*–*trans* isomerizable ligand at a given geometric conformation was effective, preventing further isomerization, thus allowing the distinction of each one of the isomers in the photolysed mixture. In addition, the experimental drift times were related to the calculated surface areas of the three possible *cis*–*cis*, *cis*–*trans* and *trans*–*trans* iron(II) complex isomers. The stabilization of the ligand in a given conformation also allows us to obtain the *cis*–*cis* and *cis*–*trans* complexes exhibiting the ligand in the metastable *cis*-conformation, as well as in the thermodynamically stable *trans*-conformation.

Introduction

The photochemical *cis*-to-*trans* isomerization of double bonds, particularly of stilbene and its derivatives, has been the subject of extensive studies. The ditopic 4-{4-[2-(pyridin-4-yl)ethenyl]phenyl}-2,2':6',2''-terpyridine (vpytpy) ligand reported in this work is a new stilbene-like compound possessing an isomerizable ethylenic bridge connecting the coordinating terpyridyl and pyridyl groups (Fig. 1). This specie was synthesized in the *trans* configuration, but it is susceptible to isomerization upon light and heat absorption, as well as *via* energy transfer processes. Quantification of the relative amounts of *cis*–*trans* isomers in photolysed samples is usually accomplished by ¹H-NMR or UV-vis spectroscopy. In the latter case, superimposition of the *cis* and *trans* bands is quite common and the lack of the pure isomer spectra or molar absorptivities precludes the accuracy of the method. On the other hand, conventional chromatographic separations of such isomers in solution are laborious and time-consuming.

Ion mobility mass spectrometry (IMS) is a gas phase ion separation/identification technique capable of resolving isobaric and isomeric ions with the same mass/charge ratio (*m/z*) but exhibiting different collision cross-sections, or dipolar moments and/or polarizabilities. Several IMS configurations have already been employed to separate structural isomers, such as field asymmetric waveform (FAIMS), tandem differential mobility analysis (TDMA) and traveling wave ion mobility (TWIM);^{1–5} but, to the best of our knowledge, no report on the use of IMS in the study of *cis*–*trans* photoisomerization has yet been published.

Among IMS apparatus, travelling wave ion mobility (TWIM) has been recently introduced as a new mode of ion propulsion and separation.⁶ The isomeric resolution can be accomplished, thanks to the difference of interaction of those species with a drift gas, in a low-pressure gas chamber, by changing the ion mobilities under the influence of travelling wave electric fields.^{7,8}

Cis and *trans* isomers have been the subject of investigation by TWIM-MS. Dong *et al.*⁹ showed that geometric isomers of carotenoids can be successfully separated by TWIM-MS, although tandem mass and collision-induced dissociation (CID) fragmentation spectra of carotenoid isomers showed similar spectral patterns.^{10,11} It was found that molecules in pure all-*trans* carotenoid samples suffer *trans*-to-*cis* thermal isomerization even when mild ionization conditions, such as in electrospray sources, were employed. This in-source isomerization explains why the ESI-MS and ESI-MS/MS spectra of isomerically pure carotenoids and retinoic acid samples are almost identical to the

^aUniversity of São Paulo, Institute of Chemistry, Av. Prof. Lineu Prestes 748, CEP 05508-000 São Paulo, SP, Brazil. E-mail: sergioht@gmail.com; koiaraki@iq.usp.br; Tel: +551130918513

^bThoMSon Mass Spectrometry Laboratory, Institute of Chemistry, University of Campinas, UNICAMP 13083-970, Campinas, SP, Brazil. E-mail: eberlin@iqm.unicamp.br

† Electronic supplementary information (ESI) available. See DOI: 10.1039/c2an35320b

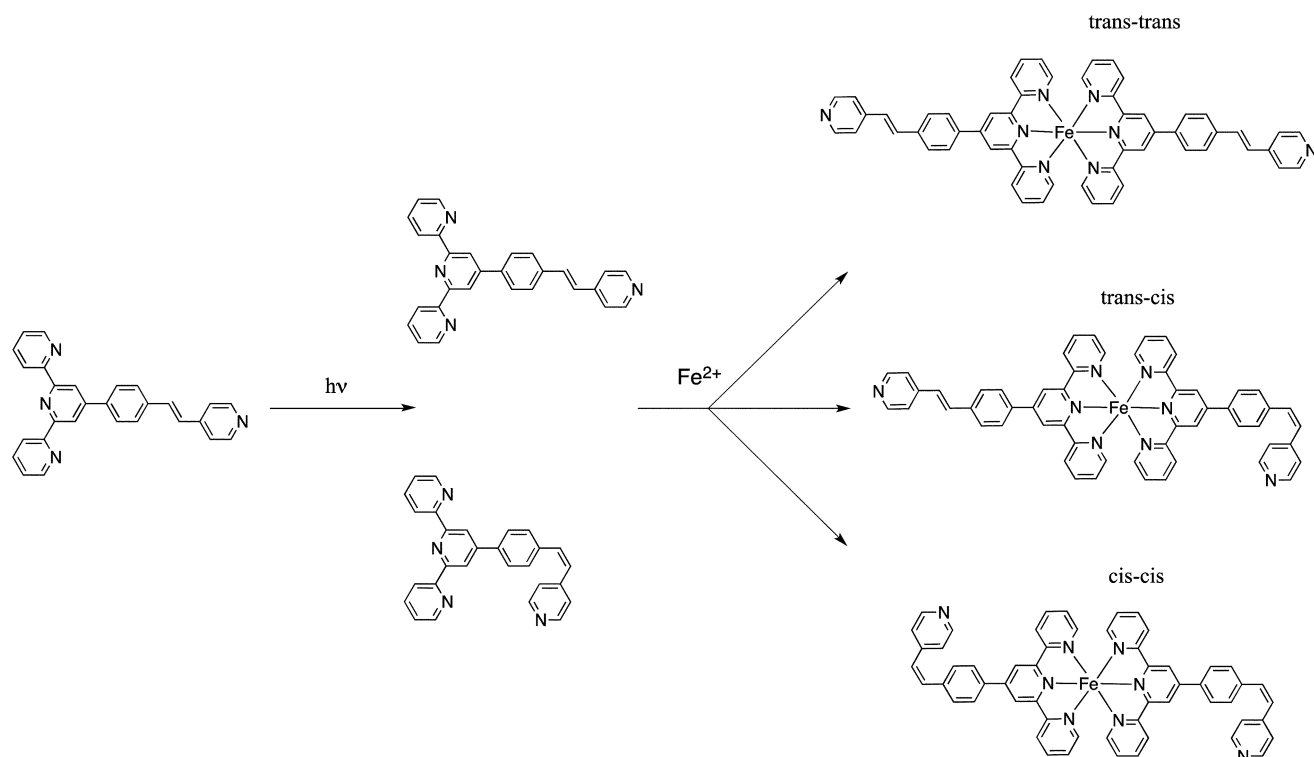


Fig. 1 Scheme showing the photoisomerization of the *trans*-vpytpy free ligand to the *cis*-configuration and the reaction with Fe(II) ions generating a mixture of *trans-trans*, *trans-cis* and *cis-cis* complexes to be probed by TWIM-MS.

spectra of mixtures of the *cis* and *trans* isomers.^{9–11} In this peculiar case, the inherent in-source isomerization of pure samples still remains a challenge for the MS analysis of mixtures of such geometric isomers.

One of the possible ways to block the isomerization process is introducing new low-lying excited states by coordination of transition metal ions. The insertion of such electronic levels can drive the excitation deactivating the isomerization pathway.

In this work, the vpytpy ligand possesses a terpyridyl group that presents high affinity for transition metal ions, particularly Fe²⁺ ions ($K_a \sim 10^{21}$). In the presence of excess of Fe²⁺ ions, the vpytpy ligand reacts quantitatively forming exclusively the [Fe(vpytpy)₂]²⁺ complexes due to the ligand field stabilization associated with the high to low spin transition.¹² In addition, complexation with Fe²⁺ ions quenches the isomerization processes of the vpytpy ligand due to the rise of low-lying excited states, driving the electronic excitation outside the isomerization pathways. Accordingly, the photoisomerization of the free *trans*-vpytpy ligand was induced by optical excitation, and the products quenched by complexation with Fe²⁺ ions, and the relative amounts of the respective *cis-cis*, *cis-trans* and *trans-trans* isomers determined by TWIM-MS, as illustrated in Fig. 1.

Experimental

Synthesis of Br-ph-tpy

The 4'-(4-bromo-phenyl)-2,2':6',2''-terpyridine intermediate, Br-ph-tpy, was obtained according to a method previously reported in the literature and purified by recrystallization in an

ethanol–water mixture.¹³ Yield = 52%. Anal. found: C, 64.5; H, 3.78; N, 10.9. Calc. for C₂₁H₁₄BrN₃ ($M_w = 388.26$): C, 64.96; H, 3.63; N, 10.82%. Observed [M + H]⁺: $m/z = 387$ and 389 .

Synthesis of *trans*-vpytpy

The 4-{4-[2-(pyridin-4-yl)ethenyl]phenyl}-2,2':6',2''-terpyridine (*trans*-vpytpy) was prepared by Heck cross-coupling reaction of 0.500 g (12.8×10^{-3} mol) of Br-ph-tpy with 0.150 g (14.2×10^{-3} mol) of 4-vinylpyridine, in the presence of 0.030 g (0.13×10^{-3} mol) of palladium acetate, 0.102 g (0.39×10^{-3} mol) of triphenylphosphine and 10 cm³ of triethylamine.^{14,15} The reaction mixture was sealed in a glass ampoule under N₂ atmosphere, heated at 120 °C for 72 h, and the crude mixture extracted with chloroform. The organic phase was washed three times with distilled water and the solvent was removed in a flash evaporator, generating a solid that was purified by recrystallization in an ethanol–water mixture.

Yield = 50%. Anal. found: C, 81.2; H, 4.95; N, 13.6. Calc. for C₂₈H₂₀N₄ ($M_w = 412.49$): C, 81.53; H, 4.89; N, 13.58%. ESI-MS: $m/z = 413.15$; calc. for [M + H]⁺ 413.18.

Preparation of *cis*-vpytpy and [Fe(vpytpy)₂]²⁺ complex

The *trans*-vpytpy ligand was converted to the *cis*-isomer by 355 nm UV-light irradiation. A 3 mL sample of a 1.0×10^{-2} mol L⁻¹ *trans*-vpytpy methanolic solution was transferred to a quartz cuvette, purged with argon and irradiated with UV light. During the photolysis, 15 μL aliquots were taken (at 0, 20, 40, 60, 80, 120, 160 and 220 minutes), diluted to 5 mL with methanol and analysed by UV-vis and TWIM-MS. After that, to 2.5 mL of each sample were

added 10 μL of a $1.0 \times 10^{-1} \text{ mol L}^{-1} \text{ Fe}(\text{NH}_3)(\text{SO}_4)_2 \cdot 6\text{H}_2\text{O}$ solution and analysed by UV-vis and TWIM-MS.

Instrumentation

UV-vis spectra were recorded on a HP8453A diode array spectrophotometer (Hewlett-Packard) using a $3.0 \times 10^{-5} \text{ mol L}^{-1}$ solution of vpytpy and $1.5 \times 10^{-5} \text{ mol L}^{-1}$ solution of $[\text{Fe}(\text{vpytpy})_2]^{2+}$ complex in methanol. $^1\text{H-NMR}$ spectra were recorded on a 300 MHz Bruker DPX300 or a Varian Gemini 200 MHz spectrometer, using $1.0 \times 10^{-2} \text{ mol L}^{-1}$ solution of the free ligand in deuterated dimethylsulfoxide. Chemical shifts were present in ppm relative to TMS standard. Photoisomerization assays were conducted using an Oriel model 74009 monochromator, set at 355 nm, as a light source. The light intensity at the sample position was calibrated with an iron(III)-oxalate actinometer.

TWIM-MS measurements

Travelling wave ion mobility mass spectrometry (TWIM-MS) data were collected using a first generation Synapt HDMS (high-definition mass spectrometer; Waters Corp., Manchester, UK) equipped with an ESI source and a hybrid quadrupole ion mobility orthogonal acceleration time-of-flight (oa-TOF) geometry. In our instrument, the TWIM cell entrance and exit apertures were reduced from 2 mm to 1 mm diameter to allow more efficient control of the drift gas pressure up to 1 mbar without any significant detrimental effect on MS performance. Methanolic solutions of the samples were submitted to ESI(+), the ions of interest were then mass selected in the quadrupole analyzer and transferred to the TWIM cell, operated at 1.45 mbar of CO_2 , with the following wave parameters: 180 m s^{-1} wave velocity and 30 V wave height.

Results and discussion

Photoisomerization of the vpytpy ligand

Vpytpy possesses a mono- and a tricoordinating site in opposite positions connected by an isomerizable ethylenic group. Stilbene-like compounds constitute an important class of photoactive molecules and one of the best-known *cis/trans* isomerization model systems.^{16–22} Its most characteristic feature is the ability to undergo photoisomerization either as isolated molecules in gas-phase or as solvated molecules in organic and aqueous solutions.¹⁶ On UV-light irradiation, stilbene is promoted to the S_1 excited-state with a C=C bond order smaller than the ground state species, thus accounting for the free rotation around the ethylenic bridge within its short lifetime.

According to Waldeck,¹⁶ there are three possible mechanisms for the photochemical conversion of the *trans*- to the *cis*-isomer. The first, and less probable, mechanism involves the non-radiative decay of S_1 to highly excited vibrational levels of the ground electronic state susceptible to isomerization, in analogy to thermally induced processes. The second mechanism involves the intersystem crossing and isomerization of the molecule in the lowest excited triplet state, at the crossing point with the ground singlet pathway responsible for the *trans* to *cis* conversion. The third and most commonly accepted mechanism involves the

so-called phantom state $p^{*16,23}$ because of its very short lifetime of about 1 ps. The phantom state can be reached from both, electronically excited *trans* and *cis* states, as a consequence of a 90° twisting of the C=C bond around its axis (Fig. 2A). The deactivation of this state leads to statistical formation of *cis* and *trans* isomers. Intersystem crossing from the singlet S_1 excited-state to a triplet excited-state can be neglected at room temperature, in the condensed phase, such that only the singlet state can be considered. However, the fluorescence decay from this state cannot be neglected. Interestingly, *trans*-stilbene is much more fluorescent ($\Phi_{\text{fl}} = 0.035$, in *n*-pentane)²⁴ than the corresponding *cis*-isomer ($\Phi_{\text{fl}} = \sim 9 \times 10^{-5}$),²⁵ and exhibits some solvent and temperature dependence.

The UV-vis spectrum of pure *trans*-vpytpy is dominated by an intense absorption band at 326 nm, ascribed to an intra-ligand (IL) transition. This faded upon irradiation with 355 nm light while the absorption increased at 285 nm defining an isosbestic point at 298 nm (Fig. 3), as expected for the *trans*-to-*cis* photoisomerization. The quantum yield Φ_{iso} of this process was determined to be 0.22. This is comparable to the photo-isomerization quantum yield determined for *trans*-1,2-bis(4-pyridyl)

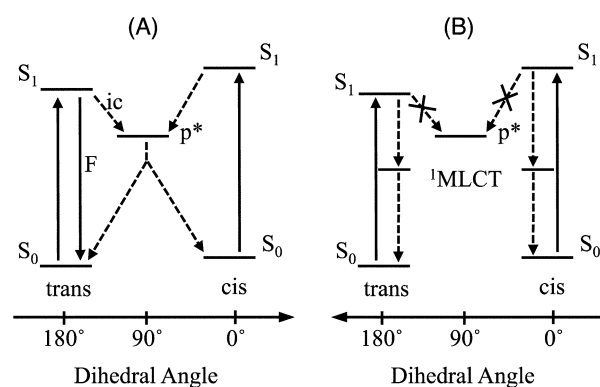


Fig. 2 Schematic energy diagram for the photo-isomerization of vpytpy as free ligand (A) and in the $[\text{Fe}(\text{vpytpy})_2]^{2+}$ complex (B). The intersystem crossing is facilitated in the complex but is not shown for clarity.

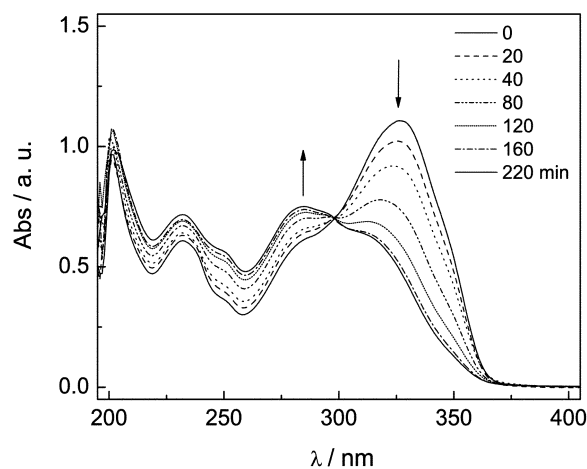


Fig. 3 Overlay of a set of UV-vis spectra registered for a $3.0 \times 10^{-5} \text{ mol L}^{-1}$ solution of *trans*-vpytpy in methanol as a function of the irradiation time with 355 nm light.

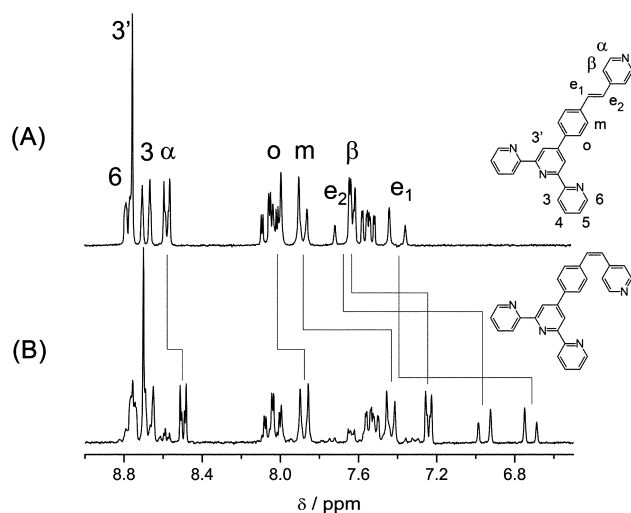


Fig. 4 $^1\text{H-NMR}$ spectrum of *trans*-vpytpy in dmsO-d_6 , (A) before and (B) after irradiation with 355 nm light and conversion to *cis*-vpytpy.

ethylene in the same solvent ($\Phi_{\text{iso}} = 0.17$),²⁶ but is lower than that reported for *trans*-4-styrylpyridine in *n*-hexane ($\Phi_{\text{iso}} = 0.37$) and acetonitrile solution ($\Phi_{\text{iso}} = 0.46$).²⁷ This behavior can be accounted for by a higher contribution of the ethenyl π^* orbitals to the S_1 state, thus weakening the $\text{C}=\text{C}$ π -bond to a larger extent.

The photo-isomerization reaction of *trans*-vpytpy in methanol solution upon irradiation with 355 nm light was confirmed by $^1\text{H-NMR}$ spectroscopy (Fig. 4). The signals were assigned by careful comparison with the $^1\text{H-NMR}$ spectra of related terpyridine derivatives, and confirmed by the $^1\text{H-}^1\text{H}$ COSY 2D correlation spectra of the *trans* and *cis*-isomers (Fig. S1†). The irradiation led to the up-field shift of e_1 and e_2 signals of the styrylpyridyl moiety whereas the terpyridyl signals remained practically unchanged, except for the $\text{H}_{3'}$ proton signal which experienced a 10 Hz up-field shift. The signals at 7.67 and 7.39 ppm, assigned to the ethylenic protons, were shifted to 6.86 and

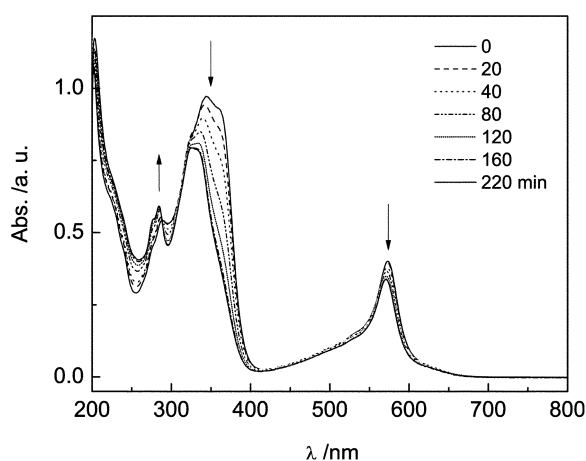


Fig. 5 Set of UV-vis absorption spectra of the $[\text{Fe}(\text{vpytpy})_2]^{2+}$ complex as a function of the irradiation time (0 to 220 min) with 355 nm light. The complex was generated *in situ* by reacting a methanolic solution of $\text{Fe}(\text{II})$ and *trans*-vpytpy.

6.72 ppm respectively, and their coupling constants decreased from 16.5 to 12 Hz confirming the *trans* (A) to *cis* (B) isomerization process (Fig. 4).

The photoisomerization of stilbene-like ligands can be suppressed by quenching the excited-state localized on the $\text{C}=\text{C}$ bond. In the case of vpytpy, this can be easily achieved by coordination of suitable transition metal ions, such as d_6 $\text{M}(\text{II})$ ions exhibiting low-lying MLCT states able to deactivate the intraligand excited state (IL^*) responsible for the photo-isomerization reaction. Iron(II) is one of the best candidates among them since the $[\text{Fe}(\text{vpytpy})_2]^{2+}$ complex has a very high formation constant and a low energy MLCT electronic state (Fig. 5). That 1 : 2 complex is so stable that it is preferentially formed even in the presence of a large excess of iron(II) ion. In fact, the global formation constant β_2 ($\log \beta_2 \approx 21$) is about 7 orders of magnitude larger than β_1 ($\log \beta_1 \approx 14$). This is explained by the ligand field stabilization of metal ion t_{2g} orbitals as a consequence of strong metal-to-ligand ($d-\pi^*$) back-bonding interaction and the dynamic chelate effect,²⁸ changing the spin state from high to low spin upon coordination of the second vpytpy ligand.

Fig. 5 shows the absorption spectra of the $[\text{Fe}(\text{trans-vpytpy})_2]^{2+}$ complex as a function of the irradiation time. A small decrease of the 570 nm MLCT band intensity is apparent, but the main changes occurred in the terpyridine IL envelope around 320 nm. The absorption of the *trans*-vpytpy species, centered at 344 nm, diminished whereas the absorption at 284 nm increased. It is not possible, however, to distinguish the *trans-trans*, *trans-cis* and *cis-cis* isomeric complexes exclusively based on the UV-vis spectra.

TWIM-MS

Fig. 6 shows the TWIM-MS of pure *trans*-vpytpy (protonated molecules of m/z 413) before and after irradiation at 355 nm.

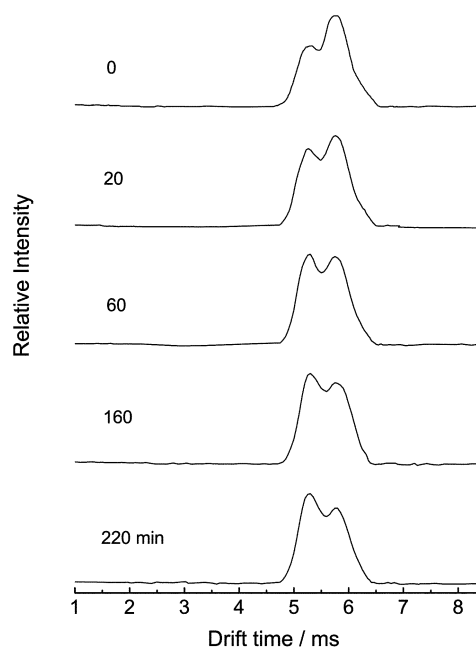


Fig. 6 Evolution of TWIM-MS drift time plots of vpytpy ligand as a function of the irradiation time (0 to 220 min) with 355 nm light, showing the change in the distribution of the *cis* and *trans* isomers ($[\text{M} + \text{H}]^+$ of m/z 413).

Note the presence of two peaks at 4.3 and 4.8 ms, even in the non-irradiated sample (Fig. 6, top), clearly indicating the presence of a mixture of two isomeric species with the same m/z .

Upon irradiation, the first peak increased as the second decreased until eventually inverting their relative abundances. It is evident that the species with the lower mobility is being photoconverted to the one with higher mobility, as expected for the *trans*-to-*cis* isomerization. The presence of the *cis*-isomer was not however expected in the non-irradiated sample, since the sample was previously confirmed to be pure by spectroscopic and TLC analyses. Similar results were previously reported for pure all-*trans* lycopene and β -carotene and extensively studied by HPLC and LC-IM-MS, showing that in-source thermal isomerization takes place prior to the analysis by TWIM-MS.⁹ Unfortunately, that process could not be avoided even under the mildest conditions, for example by decreasing the temperature of desolvation. For this particular system, it would be interesting if such isomerization processes could be suppressed, thus allowing the resolution and quantitative analyses of mixtures of *cis*-*trans* isomers by TWIM-MS.

Indeed, after coordination of vpytpy to iron(II), no photoisomerization could be observed, demonstrating the complete suppression of the phantom p^* state.

Fortunately, the TWIM-MS behavior of the $[\text{Fe}(\text{trans-vpytpy})_2]^{2+}$ complex was completely different from that shown in

Fig. 7 for the free ligand. In fact, only one sharp peak was observed at 4.37 ms in the TWIM-MS of the mass selected doubly charged ion with m/z 441 ($\Delta m/z$ of isotopologue ions = 0.5) obtained by the reaction of pure *trans*-vpytpy ligand with Fe(II). This single peak is a clear indication that the *cis*-*trans* isomerization process of vpytpy taking place in-source was suppressed by that transition metal ion. The ligand S_1 excited-state should be suppressed mainly by the low lying singlet MLCT state (Fig. 2), but also by intersystem crossing to the triplet states that is significantly enhanced in the Fe(II) complex. The successful suppression of the *cis*-*trans* isomerization process motivated us to go forward and study the possibility of analyzing the relative amounts of the three geometric isomers of the $[\text{Fe}(\text{vpytpy})_2]^{2+}$ complex (Fig. 1) that can be formed by the reaction of Fe(II) with mixtures of *cis*- and *trans*-vpytpy, as those generated from a pure *trans*-vpytpy solution as a function of the irradiation time (Fig. 7).

Interestingly, the intensity of the sole peak at 4.37 ms, assigned to the *trans*-*trans* $[\text{Fe}(\text{vpytpy})_2]^{2+}$ species, decreased in the sample prepared with the free ligand irradiated for 20 min and a new peak appeared at 4.05 ms. In fact, the 4.05 ms peak increased at the expense of the 4.37 ms peak as a function of the photoisomerization time of the free *trans*-vpytpy ligand, reaching a maximum at about 40 min of irradiation. This was followed by the decrease of that second peak and the rise of a third peak at

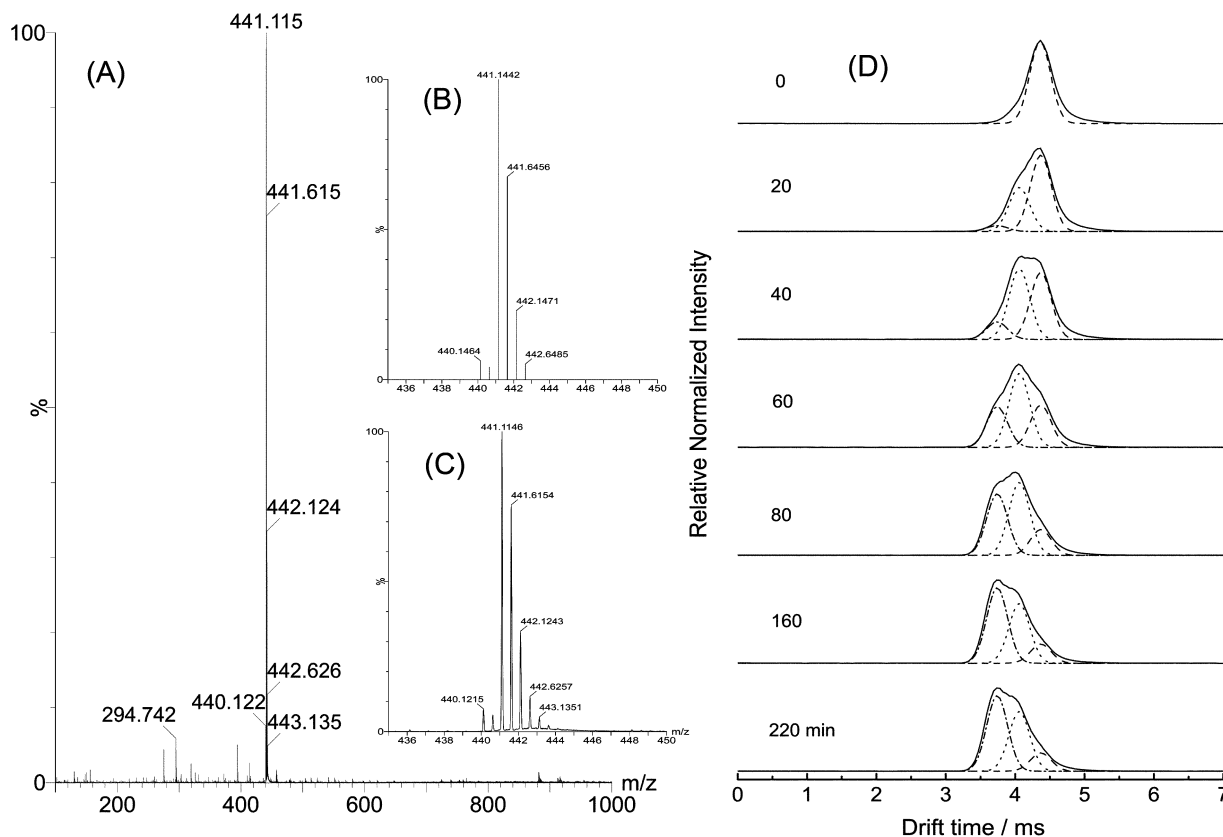


Fig. 7 (A) ESI-MS spectrum of the $[\text{Fe}(\text{trans-vpytpy})_2]^{2+}$ solution. (B) Theoretical and (C) experimental isotopologue ratios of $[\text{Fe}(\text{trans-vpytpy})_2]^{2+}$. (D) TWIM-MS drift time plots showing the mixtures of the *cis*-*cis* (dashed-dotted, 3.74), *cis*-*trans* (dotted, 4.07) and *trans*-*trans* (dashed, 4.37 ms) isomers of the $[\text{Fe}(\text{vpytpy})_2]^{2+}$ complex generated by the reaction of Fe^{2+} with non-irradiated and irradiated (355 nm) *trans*-vpytpy as a function of time. The peaks corresponding to each geometric isomer were deconvoluted using Gaussian curves.

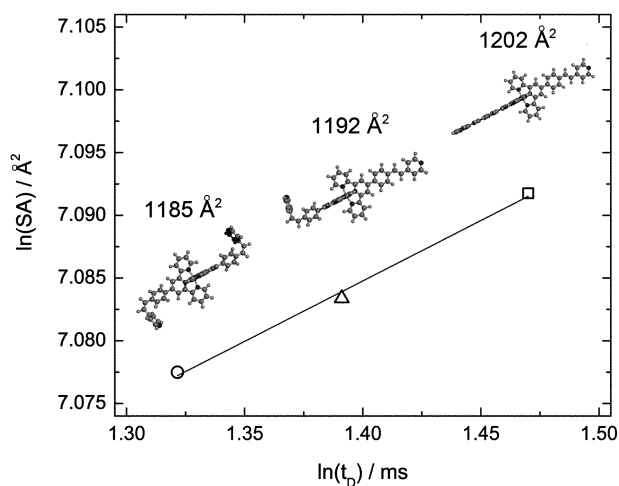


Fig. 8 Logarithmic plot of the calculated surface area of the three $[\text{Fe}(\text{vpytpy})_2]^{2+}$ complex isomers (*cis-cis* ○; *trans-cis* △; *trans-trans* □ complexes) versus the respective drift time.

3.74 ms, that become the most prominent one for samples prepared with the ligand irradiated for longer than ~ 60 minutes (Fig. 7). However, no further change could be observed for irradiation periods longer than 220 min.

At this point, it is important to note that statistical mixtures of the geometric isomers of the $[\text{Fe}(\text{vpytpy})_2]^{2+}$ complex are expected when mixtures containing different proportions of *cis* and *trans*-isomers of the vpytpy ligand are reacted with $\text{Fe}(\text{II})$. Therefore, the relative amounts of *trans-trans*, *trans-cis* and *cis-cis* species should be governed by the free vpytpy ligand *cis/trans* ratio prior to the coordination reaction, if one considers that the coordinating properties of the terpyridyl group are preserved and no further isomerization takes place after formation of the complex. Accordingly, when the *trans*-vpytpy solution is irradiated for a short period of time, the relative amount of the *cis*-isomer should be quite small leading almost exclusively to *trans-trans* and *trans-cis* isomers. Thus, the peaks at 4.37 and 4.05 ms (Fig. 7) can be assigned, respectively, to those species. Indeed, the *last* isomer is expected to present a lower collision cross-section than the *trans-trans* complex, and consequently

higher mobility in the gas phase. In contrast, the relative amounts of the *cis-vpytpy* isomer should prevail at longer periods of irradiation, favoring the formation of *cis-cis* and *trans-cis* complexes. The mobility of the *cis-cis* complex in the gas phase is expected to be even higher as confirmed by the peak at 3.74 ms in the TWIM-MS, because of its significantly much smaller collision cross-section.

Usually, the experimental collision cross-section of a given molecule is determined based on a calibration curve generated by measuring the gas phase mobility of standard compounds (drift gas pressure, flow rate, ESI conditions, wave velocity and ramping) and comparing with the mobility of an unknown species under the same experimental conditions.^{9,29} Theoretical collision cross-sections can also be evaluated using molecular modelling software, after molecular geometry optimization.

According to Smith *et al.*,⁷ the relationship between the collision cross-section (Ω) and the ion mobility in TWIM-MS measurements can be expressed by eqn (1),

$$\Omega = \frac{(18\pi)^{1/2}}{16} \frac{ze}{(K_b T)^{1/2}} \left[\frac{1}{m_i} + \frac{1}{m_N} \right]^{1/2} \frac{760}{P} \frac{T}{273.2} \frac{1}{N} A t_D^B \quad (1)$$

where t_D is the drift time, z is the number of charges on the ion, e is the charge of an electron (1.6022×10^{-19} C), K_b is the Boltzmann constant and P , T and N are the drift gas pressure, temperature and number of density, respectively. The term $(1/m_i + 1/m_N)$ is the reciprocal of the reduced molecular mass of the ion (m_i) and the drift gas (m_N). The travelling wave characteristics are expressed by the constants A and B , where the first is a correction factor for electric field parameters and the second compensates for the non-linear effects of a given TWIM device. Conveniently, the collision cross-section can be expressed as a quantity (Ω') independent of the mass and charge by multiplying Ω (eqn (1)) by the absolute charge (ze) and $(1/m_i + 1/m_N)^{1/2}$, thus giving eqn (2):

$$\Omega' = \frac{(18\pi)^{1/2}}{16} \frac{1}{(K_b T)^{1/2}} \frac{760}{P} \frac{T}{273.2} \frac{1}{N} A t_D^B \quad (2)$$

or

$$\Omega' = A' t_D^B \quad (3)$$

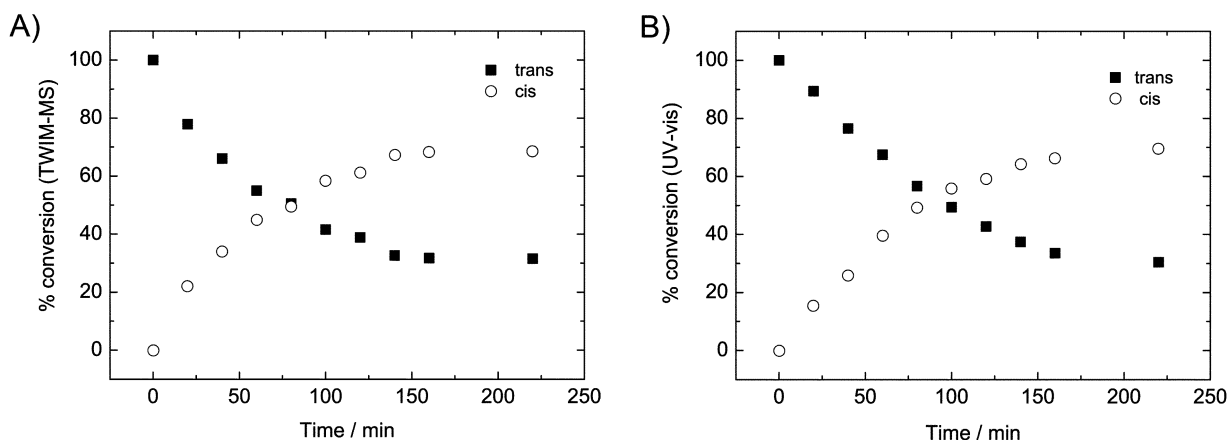


Fig. 9 Kinetic of the *trans* to *cis* isomerization (A) based on TWIM-MS and (B) UV-vis spectrophotometric data.

where A' is a constant combining all eqn (2) parameters kept unchanged in the experiments, *i.e.* temperature, pressure, density and electric field. Thus, there should be a linear relationship between the collision cross-section and the drift time of a series of isomeric ions (eqn (3)).

To confirm that correlation, the experimental drift times of the *trans-trans*, *trans-cis* and *cis-cis* isomers can be correlated with a geometric parameter reflecting Ω , such as the surface area of those complexes. This was calculated using the HyperChem™ 7.1 software, after geometry optimization at the PM3 level. The logarithm of the calculated surface areas ($\ln(\text{SA})$) was shown to be a linear function of the logarithm of the respective drift times ($\ln(t_D)$), confirming the validity of eqn (3) (Fig. 8). This result also supports the assignment of the TWIM-MS peaks at 3.74, 4.05 and 4.37 ms to the *cis-cis*, *trans-cis* and *trans-trans* isomers of the $[\text{Fe}(\text{vpytpy})_2]^{2+}$ complex.

The photoisomerization kinetics of *trans-vpytpy* were monitored by UV-vis spectrophotometry and TWIM-MS following the decay of the IL absorption band at 350 nm (Fig. 9B) and the integrated area of the deconvoluted drift time peaks. Single saturation curves, in which the point corresponding to a 1 : 1 mixture of *cis* and *trans*-isomers was achieved after 75 min of irradiation and reached saturation after about 200 min, were obtained spectrophotometrically. A very similar result was obtained when the integrated areas of the deconvoluted TWIM-MS peaks (see Fig. 7) of the same set of samples were plotted as a function of the irradiation time (Fig. 9A), clearly indicating that there is no significant isomerization at the ESI source. In fact, the apparent rate constants evaluated by TWIM-MS and UV-vis data were in good agreement, *i.e.* $(71 \pm 1) \times 10^{-4}$ and $(69 \pm 3) \times 10^{-4} \text{ min}^{-1}$, respectively.

Conclusions

The *cis-trans* isomerization of the 4-{4-[2-(pyridin-4-yl)ethenyl]phenyl}-2,2':6',2''-terpyridine ligand (vpytpy) was shown to be suppressed by coordination to iron(II) ion forming the $[\text{Fe}(\text{vpytpy})_2]^{2+}$ complex. This ligand stabilization in a given (*cis* or *trans*) conformation is a consequence of the presence of a low lying MLCT electronic excited state that efficiently quenches the higher energy phantom p^* state, as well as the presence of several low energy vibrational states created by the formation of the complex preventing the molecule from reaching the crossing point for isomerization. The coordination induced “freezing” of a *cis-trans* isomerizable ligand in a given conformation was shown to be an interesting and efficient strategy to avoid in-source isomerization during ESI, thus allowing the analyses of mixtures of geometric isomers by TWIM-MS. Also, the experimental drift times determined by TWIM-MS were shown to be proportional to the calculated surface areas of the isomeric complexes. The stabilization of the ligand in the respective conformation should allow the preparation of the *cis-cis* and *cis-trans* complexes in which the ligand is in the metastable *cis*-conformation, as well as in the thermodynamically stable *trans*-conformation.

Acknowledgements

The authors are grateful to Fundação de Amparo à Pesquisa do Estado de São Paulo (FAPESP) and Conselho Nacional de Desenvolvimento Científico e Tecnológico (CNPq) for the financial support.

Notes and references

- 1 B. M. Kolakowski and Z. Mester, *Analyst*, 2007, **132**, 842–864.
- 2 G. Papadopoulos, A. Svendsen, O. V. Boyarkin and T. R. Rizzo, *Faraday Discuss.*, 2011, **150**, 243–255.
- 3 M. Bilde and S. N. Pandis, *Environ. Sci. Technol.*, 2001, **35**, 3344–3349.
- 4 P. M. Lalli, B. A. Iglesias, D. K. Deda, H. E. Toma, G. F. de Sa, R. J. Daroda, K. Araki and M. N. Eberlin, *Rapid Commun. Mass Spectrom.*, 2012, **26**, 263–268.
- 5 M. Benassi, Y. E. Corilo, D. Uria, R. Augusti and M. N. Eberlin, *J. Am. Soc. Mass Spectrom.*, 2009, **20**, 269–277.
- 6 H. Borsdorf and G. A. Eiceman, *Appl. Spectrosc. Rev.*, 2006, **41**, 323–375.
- 7 D. P. Smith, T. W. Knapman, I. Campuzano, R. W. Malham, J. T. Berryman, S. E. Radford and A. E. Ashcroft, *Eur. J. Mass Spectrom.*, 2009, **15**, 113–130.
- 8 C. S. Creaser, J. R. Griffiths, C. J. Bramwell, S. Noreen, C. A. Hill and C. L. P. Thomas, *Analyst*, 2004, **129**, 984–994.
- 9 L. L. Dong, H. Shion, R. G. Davis, B. Terry-Penak, J. Castro-Perez and R. B. van Breemen, *Anal. Chem.*, 2010, **82**, 9014–9021.
- 10 L. Q. Fang, N. Pajkovic, Y. Wang, C. G. Gu and R. B. van Breemen, *Anal. Chem.*, 2003, **75**, 812–817.
- 11 Y. Wang, W. L. Chang, G. S. Prins and R. B. van Breemen, *J. Mass Spectrom.*, 2001, **36**, 882–888.
- 12 S. H. Toma, J. J. Santos, R. G. Velho, M. Nakamura, H. E. Toma and K. Araki, *Electrochim. Acta*, 2012, **66**, 287–294.
- 13 C. B. Smith, C. L. Raston and A. N. Sobolev, *Green Chem.*, 2005, **7**, 650–654.
- 14 A. J. Amoroso, J. P. Maher, J. A. McCleverty and M. D. Ward, *J. Chem. Soc., Chem. Commun.*, 1994, 1273–1275.
- 15 A. J. Amoroso, A. M. W. C. Thompson, J. P. Maher, J. A. McCleverty and M. D. Ward, *Inorg. Chem.*, 1995, **34**, 4828–4835.
- 16 D. H. Waldeck, *Chem. Rev.*, 1991, **91**, 415–436.
- 17 A. Momotake and T. Arai, *J. Photochem. Photobiol., C*, 2004, **5**, 1–25.
- 18 F. D. Lewis, *Acc. Chem. Res.*, 1979, **12**, 152–158.
- 19 J. Saltiel and J. T. D'Agostino, *J. Am. Chem. Soc.*, 1972, **94**, 6445–6456.
- 20 J. Saltiel, G. R. Marchand, E. Kirkorkaminska, W. K. Smothers, W. B. Mueller and J. L. Charlton, *J. Am. Chem. Soc.*, 1984, **106**, 3144–3151.
- 21 J. Saltiel and Y. P. Sun, *J. Phys. Chem.*, 1989, **93**, 6246–6250.
- 22 D. Schultefrohlinde, H. Blume and H. Gusten, *J. Phys. Chem.*, 1962, **66**, 2486–2491.
- 23 J. Saltiel, *J. Am. Chem. Soc.*, 1967, **89**, 1036.
- 24 J. L. Charlton and J. Saltiel, *J. Phys. Chem.*, 1977, **81**, 1940–1944.
- 25 J. Saltiel, A. S. Waller and D. F. Sears, *J. Photochem. Photobiol., A*, 1992, **65**, 29–40.
- 26 N. Y. M. Iha, M. K. Itokazu, A. S. Polo, D. L. A. de Faria and C. A. Bignozzi, *Inorg. Chim. Acta*, 2001, **313**, 149–155.
- 27 N. Y. M. Iha, A. S. Polo, M. K. Itokazu, K. M. Frin and A. O. D. Patrocínio, *Coord. Chem. Rev.*, 2006, **250**, 1669–1680.
- 28 U. Schubert, H. Hofmeier and G. R. Newkome, *Modern Terpyridine Chemistry*, Wiley-VCH, Weinheim, 2006.
- 29 D. H. Russell, L. Tao, D. B. Dahl and L. M. Perez, *J. Am. Soc. Mass Spectrom.*, 2009, **20**, 1593–1602.